NAILS OF THE ROMAN LEGIONARY AT INCHTUTHIL

C. Mapelli, W. Nicodemi, R. F. Riva, M. Vedani, E. Gariboldi

This study is focused on the nails found at Inchtuthil, Perthshire (UK) dated back to 87 A.D.. The investigated nails were analyzed to characterize these objects. After the sectioning of the sample, an accurate optical microscopy examination has been performed in order to study the different structural constituents composing the microstructure. SEM-EDS analysis allowed to quantitatively characterize the chemical composition of non-metallic inclusions, while the SEM-EBSD examination revealed the crystallographic textures featuring the examined alloy. This information, coupled with the measurements of the micro-hardness suggests a new hypothesis on the plastic deformation process adopted for the realization of the observed nail.

KEY WORDS: Inchtuthil, Roman nails, carburising, non-metallic inclusions, metallography, SEM-EDS-EBSD

INTRODUCTION

The nails found at Inchtuthil, Pertshire, are one of the most interesting and consistent findings performed in the 20th century about the Roman steelmaking production[1,2,3]. The Roman fortress at Inchtuthil covered around 20.000m^2 and was probably capable of holding some 5.500 men. The nail have been found in a pit 3.6m deep and covered under 1.8m of clean beaten earth. This operation has probably been performed on 87A.D. in order to avoid that the nails can fall into hands of the Scot tribes, which prized the iron based products more than the silver and gold ones for the intrinsic potential of this material in the production of weapons and structural devices.
The total number of nails found is between 875.000 and 900.000 pieces. These are featured by different sizes as a function of the different applications and of stresses which had to be faced. Considering the large amount of the Roman nails found, these manufacts have not a large interest in the research on archeometallurgy because of their poor artistic and aesthetic value. The deep study performed by N.S. Angus et al.[4] allowed to classify the nails into six well defined classes, each identified by the overall length, the area of the shank section at the middle point of the shank, the shape of the head and its thickness.
The analysis developed in this study has been performed on a nail belonging to the class E according to the classification defined by Angus and co-workers, featured by an overall length of 38-63mm, by a circular disk head characterized by 9-16mm diameter and a square shank section. This type of nail is the one found with the highest frequencies, because 763.840 pieces have been counted and the observation has been integrated with the ones performed on another type of nail belonging to the class B as defined by Angus (overall length of 171-241mm, circular disk head shape, square shank section) carried out on 1992[5].

Carlo Mapelli, Walter Nicodemi,
Riccardo F. Riva, Maurizio Vedani, E. Gariboldi
Dipartimento di Meccanica del Politecnico di Milano
Via La Masa 34, 20156 Milano (ITALY)

EXPERIMENTAL PROCEDURE

In this experimental investigation, a nail belonging to class E has been analysed (Fig. 1). The nail has been sectioned along the shank axis and transversally cut in two coupons. After grinding and polishing the coupons have been etched by immersion in the Nital metallographic etching (0.5%HNO_3 for 100ml of ethanol) for 25s. Etching

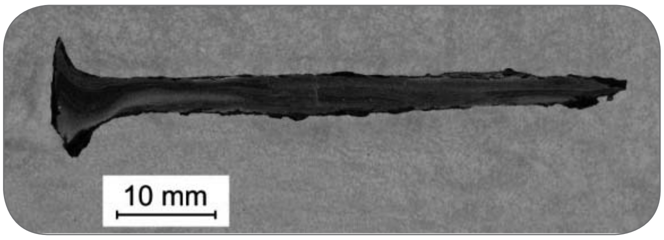

Fig. 1 **The macroscopic multi-layered aspect observed on the nail found at Inchtuthil. The clearer is the layer aspect, the higher is the perlite content of the region revealed by etching.**
Struttura a strati evidenziata dal macro-attacco in un chiodo rinvenuto presso Inchtuthil. Gli strati chiari sono quelli con maggiore presenza di perlite.

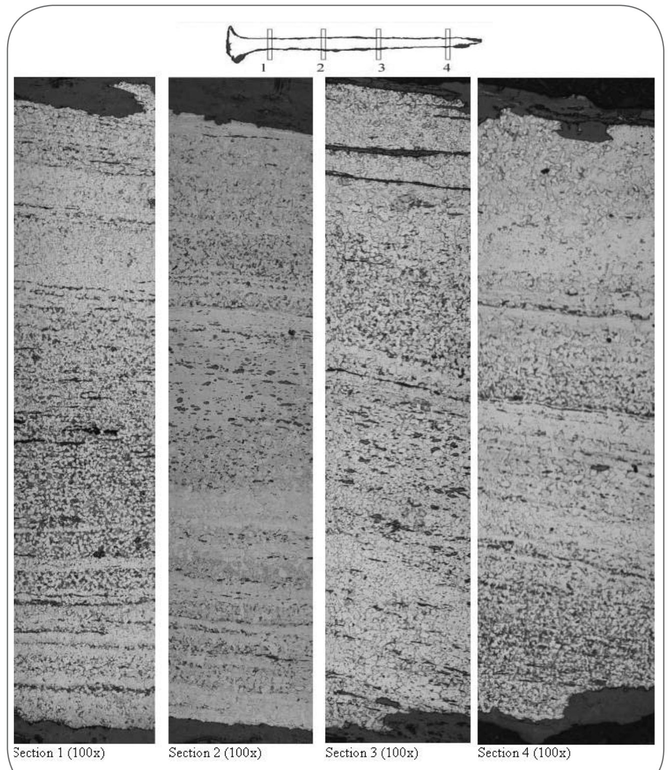

Fig. 2

Details of the layered structure.
Dettagli della struttura a strati.

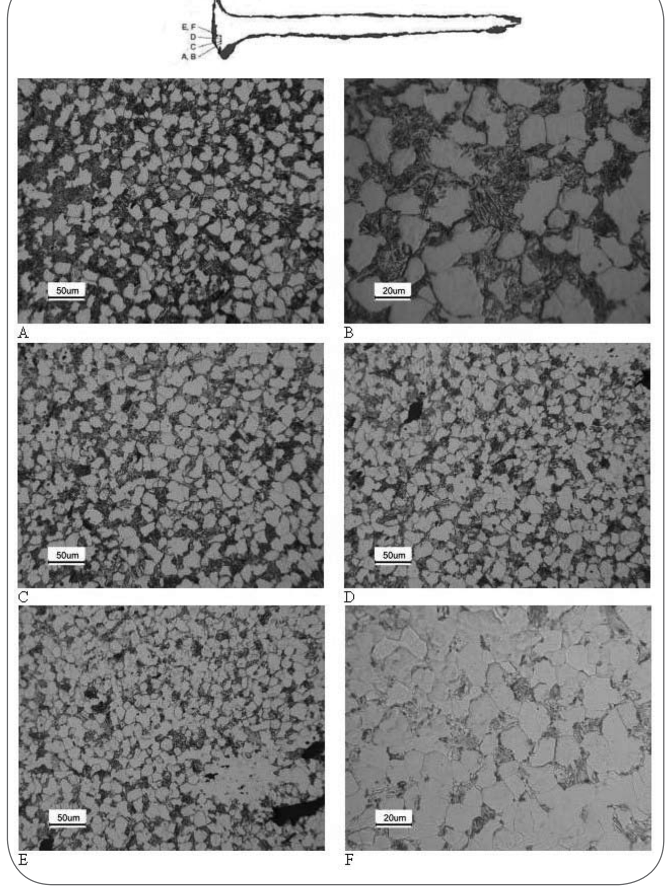

allowed to observe and distinguish the different phases by optical microscopy and the distribution of the structural constituents contained in the nail.
The chemical composition of the non-metallic inclusions has been measured by SEM-EDS technique and all the different phases revealed within them by EBS (Electron-Back-Scattering) have been chemically analysed.
The SEM-EBSD (Electron-Back-Scattering-Diffraction) analysis has been performed on two areas of the nail sections along the shank axis. The analysed areas are prevalently constituted by ferrite and are located at 10mm far from the head side and at 10mm from the nail tip. Each observed area featured by an extension of $10mm^2$ has been scanned by a pixel resolution of $2.5\mu m^2$ associated to an accelerating voltage of 20kV.
On each identified region characterized by a particular

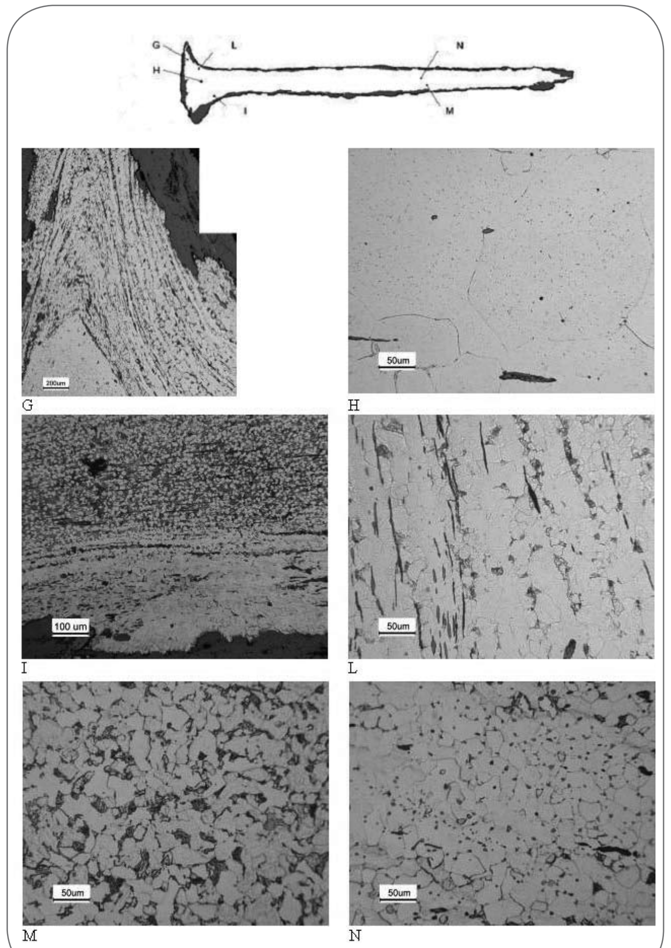

Fig. 4

Microstructures revealed in the different regions near the nail head and on the nail shank.
Microstrutture poste in evidenza nelle differenti regioni del gambo del chiodo.

Fig. 3

Microstructures revealed in the different regions near the nail head.
Microstrutture poste in evidenza nelle differenti regioni del chiodo in prossimità della testa.

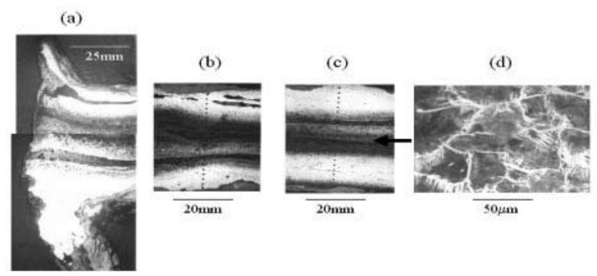

Fig. 5

Different layers revealed in nail belonging to group B: the darker is the zone the higher is the carbon content. (a) Different layers featuring the head of the nail, (b) a transversal profile of shank at 35mm from the head and (c) at 50mm from the head. (d) Particular of the acicular ferrite around the perlite grains interesting a core region of the nail.
Differenti strati posti in evidenza all'interno di un chiodo appartenente al gruppo B: le zone più scure sono quelle caratterizzate dal maggiore contenuto di carbonio. (a) Differenti strati caratterizzanti la testa del chiodo, (b) profilo trasversale del gambo del chiodo a 35mm dalla testa, (c) a 50mm dalla testa. (d) Particolare della ferrite aciculare nei pressi dei grani perlitici appartenenti alla regione interna del chiodo.

presence and distribution of the structural constituents, a micro-hardness Vickers test has been performed to point out the trend of the micro-hardness values. The micro-hardness value related to each region is the result of an averaging procedure performed on three different measurements performed with the application of a 25g load for 15s.

RESULTS

The performed metallographic etching has pointed out also the macroscopic characterization of the alternated phases (Fig.. 2, Fig. 3, Fig. 4). There is an evident presence of a layered structure indicating the phases characterised by a different carbon content.
The optical microscope observations have confirmed the presence of heterogeneous structure with the presence of ferrite and ferrite-perlite structural constituents, clearly indicating significant gradient in the carbon content of the different layers (Fig. 3, Fig. 4). This particular distribution of the structural constituents has been revealed also in the nail belonging to group B in which also a more significant presence of acicular ferrite takes place. The morphology of acicular ferrite suggests that it has been formed at the perlite boundaries as the result of pro-eutectoid formation (Fig. 5).
All the non-metallic inclusions revealed by the SEM-EBS analysis have pointed out a two-phase structure constituted by a dark matrix of fayalite ($2FeO.SiO_2$) with the presence of the clear wustite (FeO_x) phase in globular or dendritic form (Fig. 6, Fig. 7).
The textures pointed out by the SEM-EBSD showed a sharp anisotropy pattern (Fig. 8, Fig. 9) characterized by the induction of strong and clear texture revealed on the ODF diagram:
- in the shank traces of γ-fiber (from {111}<100> to

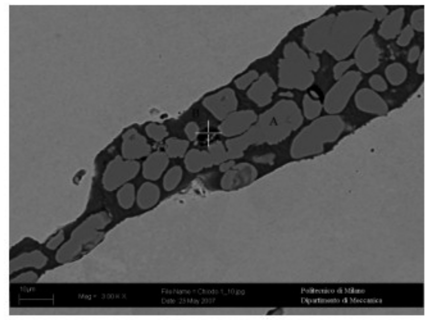

%wt	MgO	Al_2O3	SiO_2	P_2O_5	CaO	TiO_2	MnO	FeO
spot A	-	1.7	2	-	-	-	3.9	92.3

Fig. 6

Typical elongated non-metallic inclusion found in the nail and the chemical composition related to point A and point B.
Tipiche inclusioni non metalliche allungate riscontrate all'interno del chiodo. Le analisi chimiche si riferiscono ai punti indicati con A e B.

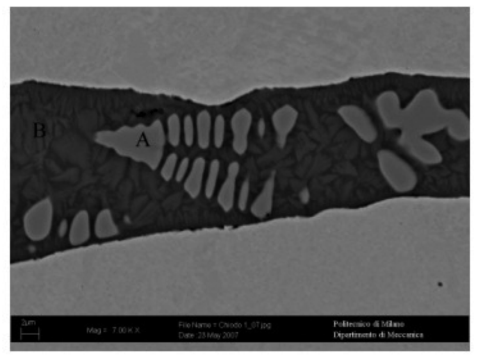

%wt	MgO	Al_2O3	SiO_2	P_2O_5	CaO	TiO_2	MnO	FeO
spot A	-	0.4	1.3	-	-	-	4.2	94.1

Fig. 7

Typical elongated non-metallic inclusion found in the nail and the chemical composition related to point A and point B. It is clear also the presence of dendritic structures related to the nucleation of FeOx from the surrounding dark matrix.
Tipiche inclusioni non metalliche allungate riscontrate all'interno del chiodo. Le analisi chimiche si riferiscono ai punti indicati con A e B. Si nota la presenza di una struttura dendritica associata alla nucleazione di FeOx a partire dalla circostante matrice scura.

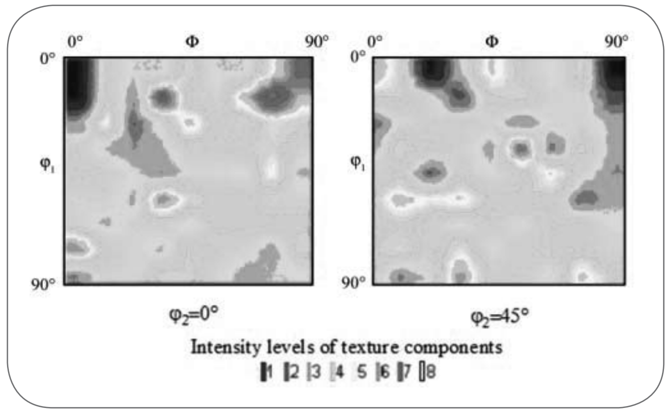

Fig. 8

The ODF diagram of the texture revealed at 10mm far from tip.

Diagramma ODF della tessitura misurata a 10mm dalla punta.

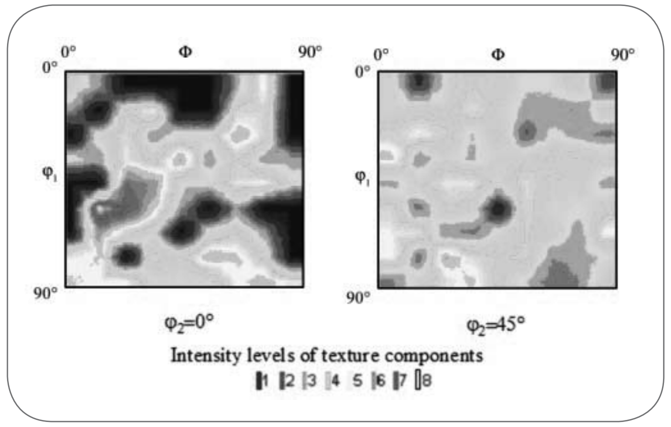

Fig. 9

The ODF diagram of the texture revealed at 10mm far from head.

Diagramma ODF della tessitura misurata a 10mm dalla testa.

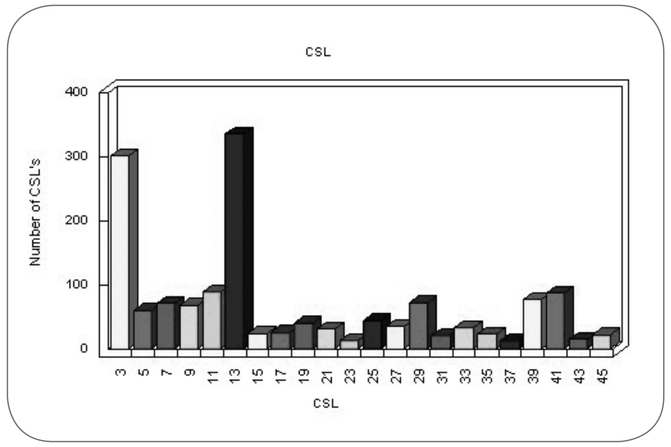

Fig. 10

The CSL recognized 10mm far from tip.

Diagramma CSL misurato a 10mm dalla punta.

{111}<101>) and of Cube component ({001}<001>) are present;
- in the region of the head a more pronounced presence of α-fiber concentrated near Goss component ({011}<100>), Cube texture ({001}<010>) and a more attenuated presence of the γ-fiber has been pointed out.

The misorientation of the grain boundary and the analysis performed through the Coincidence Site Lattice formalism reveal a situation in which the identification of strong CSL $\Sigma 3$ strongly associated with $\Sigma 13$ is easy to be recognized (Fig. 10, Fig. 11). While the misorientation grain boundary pattern reveals a different concentration on the lowest values of the misorientation boundary angles between the analysed zone adjacent the head and the tip regions (Fig. 12, Fig. 13). Particularly, it is evident that the values of the misorientation angles of the head show a lower concentration of the misorientation around the lowest boundary angles, but this is probably due only to the anomalous grain growth characteristic of this analysed regions.

The micro-hardness measurements have shown a variation in the range from 104HV (in the region prevalently featured by the presence of ferrite grains) to 135HV (in the zones characterized by the highest observed volume fraction of perlite colonies) in the nail belonging to group E while in the one of group B there is a higher average value of the measured micro-hardness and also a larger difference between the examined zones from 150HV in the ferrite region to 389HV in the perlite one (Tab. 1, Tab. 2).

DISCUSSION

The multi-layered structure by which the nail is made is confirmed by the observation of the different sections along the nail shank (Fig. 1, Fig. 2).

The layers characterized by high perlite content are present also in the core of nail and near the head, the perlite colonies assumed a significant deflection due to the plastic deformation, carried out by Roman blacksmiths to shape the head. One of the main point to be clarified for a correct interpretation of the observed structure is the comprehension of the technique followed to realize such an heterogeneous structure due to the superimposition of layers having different chemical composition. The different hypothesis can be summarized:
- the nail has been obtained by the carburation during the forging process of mild low carbon steel;
- the nail has been obtained by a bloom heterogeneously enriched in carbon during the ore reduction processes;
- the nail has been obtained by the pressure-diffusion welding of layers having a different carbon content.

The first hypothesis does not seem to be realistic since, as previously indicated, the carbon enriched layers are present also in the core and this does not seem to be consistent with the diffusion phenomena which can take place only from the surface layers. However, in order to obtain the observed structure the different and alternated strips have to be present also in the starting bloom and this situation is not simple to be induced. The second and the third hypothesis appear more plausible to better explain the presence of the examined structural constituents.

The second hypothesis could be plausible, but it is strange enough that the ancient artisans could obtain a structure featured by thin alternated layers with different carbon content. Moreover, this second hypothesis does not explain the very fine grain size featuring the transition region between the ferrite and perlitic regions often pointed out by the presence of evident and aligned strips of non-metallic inclusions. Moreover, the regularity and repeatability of the layers organization in a so high number of analysed nails[4,5] is difficult enough to be realized only starting from a single bloom. Actually, the volumes of the blooms interested by different carbon enrichment follow a very chaotic distribution. Maybe, the organization and disposition of the non-metallic inclusions permits to cast further light on the treated issues and integrate the content of the second hypothesis. The non-metallic inclusions are significantly elongated along the shank axis and they are not homogeneously distributed within the different layers. Actually, they are concentrated only on some layers and usually they define the boundary among layers characterized by different structural constituents or by a different grain size.

The non-metallic inclusions are constituted by fayalite ($2FeO.SiO_2$) saturated by FeO_x and this is certainly a non-metallic compound intentionally formed by the artisans in order to exploit its low melting point (1205°C for pure fayalite and 1175°C for fayalite saturated by wustite)[6,7], which permits to easily evacuate them during the hammering of the bloom reduced in solid phase. The first hammering of the bloom has certainly been operated around the melting temperature of the trapped slag as

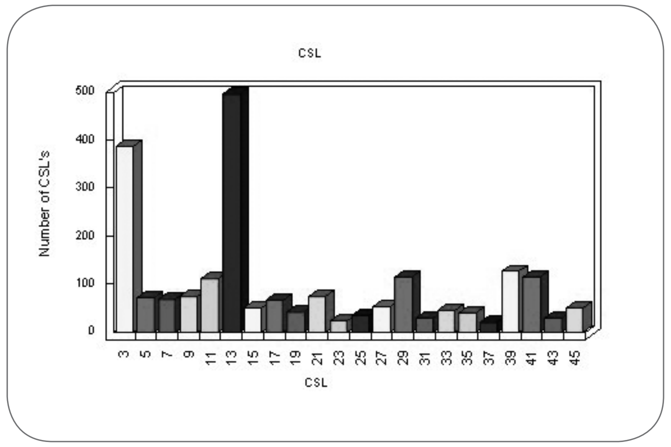

Fig. 11

The CSL recognized 10mm far from head.

Diagramma CSL misurato a 10mm dalla testa.

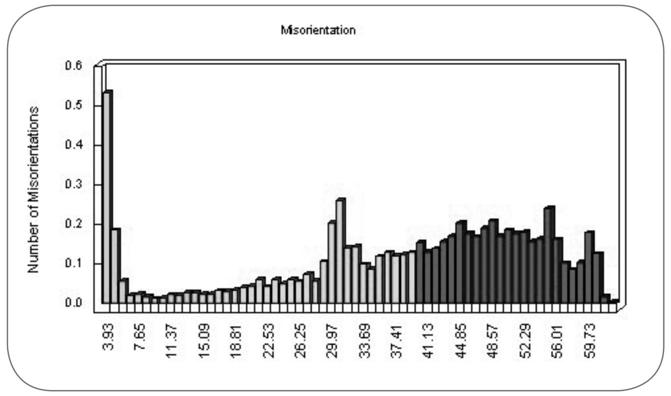

Fig. 12

The grain boundary misorientation recognized at 10mm far from tip.

Misorientazione dei bordi grano misurata a 10mm dalla punta.

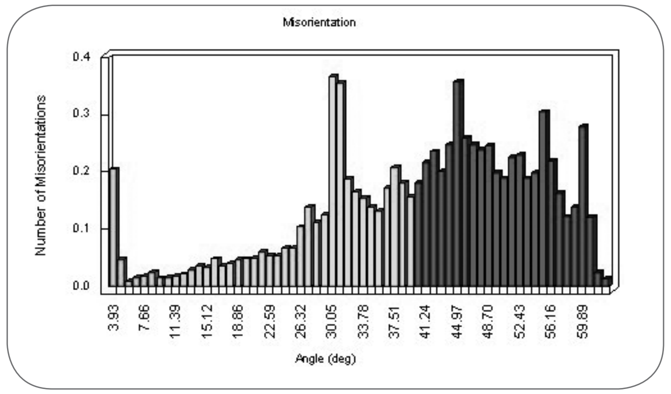

Fig. 13

The grain boundary misorientation recognized at 10mm far from head.

Misorientazione dei bordi grano misurata a 10mm dalla testa.

Zone	HV	Microstructure
Head	112	Ferrite-Perlite
Connection Head-Shank	104	Ferrite
Upper side Shank	114	Ferrite-Perlite
Lower side Shank	135	Prevalently perlite
Middle central region	108	Ferrite
Tip region	117	Ferrite-Perlite

Tab. 1

Micro-hardness measurements featuring the different zones of the nail belonging to group E.

Misure di microdurezza realizzate in diversi punti di un chiodo appartenente al gruppo E.

Zone	HV	Microstructure
Head	208	Ferrite-Perlite
Connection Head-Shank	143	Ferrite
Upper side Shank	298	Ferrite-Perlite
Lower side Shank	343	Perlite
Middle central region	389	Perlite
Tip region	272	Ferrite-Perlite

Tab. 2

Micro-hardness measurements featuring the different zones of the nail belonging to group B.

Misure di microdurezza realizzate in diversi punti di un chiodo appartenente al gruppo B.

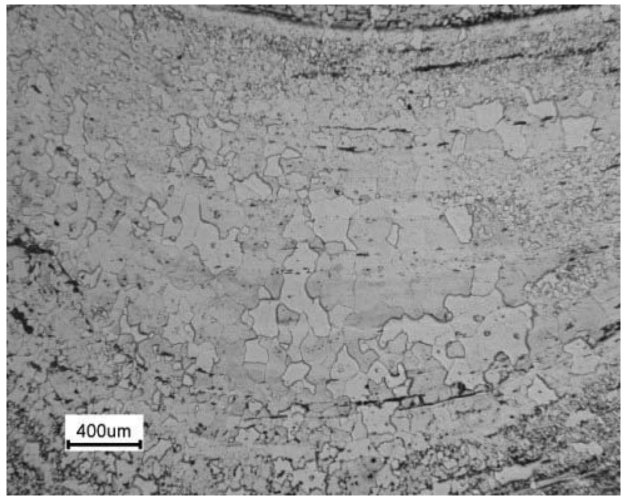

▲ *Fig. 14*

Ferrite grains characterized by abnormal growth in the head region of the nail.

Grani ferritici caratterizzati da crescita abnorme nella regione di testa del chiodo.

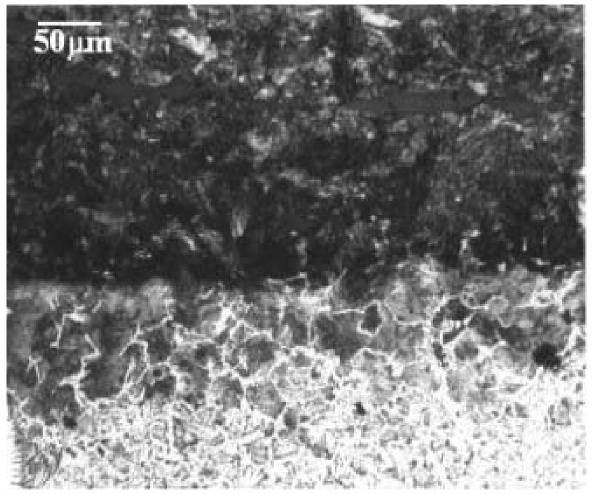

▲ *Fig. 15*

. Example of the completely perlitic layer and the region of transition from perlite grains to ferrite-perlite ones.

Esempio di strato completamente ferritico e particolare della regione di transizione tra grani ferritici e grani perlitici.

proved by the presence also of a dendritic structure of FeO_x developed in some non-metallic compounds (Fig. 6). The realization of such a slag with these characteristics and functions went on also during the Medieval Age[8]. The position of the non-metallic inclusions among the separation lines of the recognized layers has been probably realized also in order to protect the surfaces of the bloom to be welded from atmospheric oxidation. The application of a slag featured by a low-melting point seems to have been fulfilled also in other contexts[9] in order to avoid the oxidation and to permit the forge-welding[10]. Moreover, this technique, implying the coupling of very thin layers, could permit to produce a more efficient and faster carbon diffusion on these layers featured by a very little thickness. Once the layers have been thickened and chemically modified, they were welded exploiting the heat and the related atomic diffusion promoted by the friction induced by hammering. This process seems to be proved also by the little grain size featuring the region separating adjacent layers, as it is typical of the grains nucleated during the diffusion process in solid state. On the other hand, the formerly described route based on thin layers joint by friction welding seems to be complicated enough and very long-time spending. Thus, it is not possible to exclude that the blooms were intentionally or accidentally carburised on their external surfaces as a result of a prolonged contact with carbon containing substances present in the furnaces[5]. So, in order to explain the enough regular disposition of the phases within the observed nails[4,5], it is possible to formulate two different hypothesis:

- the ancient smiths started from carburized steel which has undergone a heavy decarburation of the outer surface due to the oxidation, leaving in the core the highest carbon content, but this hypothesis explains with certain difficulties the presence of structures like the one present in the previously analysed nail of Class B5), which clearly shows (within the head core phases) a ferrite strip located between two carbon enriched zones;
- it is possible to suppose that the blooms could also be flattened, enriched by carbon on outer sides and then folded back on themselves, avoiding the former realization of thin steel layers; on the other hand, this final hypothesis goes on to suppose the presence of friction welding as a fundamental stage for the consolidation of the metallic mass which has been bended and then folded back.

The texture analysis of the head regions seems to prove the occurrence of a recrystallization that partially has taken place in the austenite phase, originating the presence of intense Cube texture within the ferrite grains, while the presence of γ-fiber and of the Goss component seems to indicate that a certain quantity of the deformed austenite has been transformed in ferrite before recrystallization could take place[11]. The region of the head seems to be interested by a more intense recrystallization which has led to a less intense presence of the γ-fiber. The occurrence of a recrystallization - at least partial - seems to be proved also by the presence of the largest grain size of ferrite which appear to have undergone even a phenomenon of abnormal growth (Fig. 14). Thus, it is possible to conclude that during the shaping and finishing treatment the nail has been treated in a temperature range near the austenite-ferrite transformation and that only the head has undergone a longer permanence in this thermal range.

The analysis performed through the CSL formalism indicates the presence of a strong concentration of Σ13 boundary type, which is recognized as a type usually associated with the abnormal growth of recrystallized grains, because they are generally associated to significant grain boundary mobility[12,13]. This phenomenon is particularly evident also in the morphology of the different grains, often globular and seldom interested by a very rapid growth, particularly evident in the ferrite grains because the higher carbon concentration of the perlite grain (also precipitated under the form of Fe_3C) can act as a slowing factor for the recovery and of the following recrystallization process of the grains themselves. The misorientation analysis of the grain boundaries seems consistent with this hypothesis and the lower concentration of the boundaries on the smallest angles in the head region, appears to be due only to the lower boundary extension associated to the zones interested by the abnormal growth of the grains in this region, where the higher temperature has been probably maintained for a longer time than in the shank. Such a phenomenon can be associated to the heat developed by the plastic deformation due to the forging of the head which has probably taken place.

According to the expectations, the micro-hardness measurements have shown that these values are fundamentally ruled by the carbon content and then by the presence of perlite which increases the strength of the steel. The maximum micro-hardness reached in the nail of class B, studied in 1992[5], is much higher, because in the perlite region a maximum value of 389HV has been detected. This is certainly due to the presence of completely perlite regions intentionally formed in order to increase the strength of the nail featured by a greater size, because the larger nails were generally dedicated to undergo applications implying higher stresses (Fig. 15). This observation confirms that the ancient artisans were able to modulate the microstructure and the related properties as a function of the size of the nails and of the final applications.

CONCLUSIONS

- The analysed nail belonging to the Group E shows a composite structure featured by the simultaneous presence of ferrite colonies and perlite grains, which characterize also the nail belonging to group B featured by more extended perlite regions which provide the highest hardness value;
- the ancient blacksmiths seem to have modulated the mechanical properties as a function of the nail size which is certainly related to different applications and so to different loads;
- the non-metallic inclusions are mainly constituted by fayalite ($2FeO.SiO_2$) saturated by FeO_x. Probably, this particular formulation has been intentionally applied, because it is characterised by a low melting point of 1175°C and this certainly favours the evacuation of the slags trapped during the reduction in solid phase;
- the non-metallic inclusions often feature the bulk of a layer characterized by particular structural constituents but are always present also in the region dividing two different identified layers. The separation zones among the layers are also characterized by the presence of very small recrystallized ferrite grains which can be produced by the joining probably realized by welding operated among the different layers;
- the performed observations are plausible and consistent with the hypothesis that the method followed to produce the multi-layered structure is the welding realized by the friction developed between adjacent layers, but it is not possible at this stage to completely exclude that the multi-layered structure has been obtained by the surface decarburation of a steel initially enriched by carbon, although this last hypothesis does not well clarify some observed aspects of the microstructure;
- the crystallographic textures showed that the presence of ϒ-fiber components associated to the cube one are probably produced by a partial recrystallization of the deformed austenite;
- because the cooling rate has not been so high to produce also phases of non-equilibrium, i.e. bainite and/or martensite, it is possible to suppose that cooling of the nail has not been particularly rapid and so the reason of the difficult recrystallization of the austenite can be found in a temperature range near the austenite-ferrite transformation;
- also the high concentration of Σ3 and Σ13 CLS-type represent a clue of the presence of recrystallization that in the region of the head has been characterized by an abnormal growth of the ferrite grains, which is typical of the structure featured by Σ13, because these ones are generally associated to a very high boundary mobility;
- the micro-hardness profile of the nail belonging to group E has shown values included in the range between 104HV and 135 HV, with the maximum values associated with the presence of carbon enriched structural constituents.

The comparison among the values measured in this study and the ones formerly performed on the nail of group B (revealing higher value of hardness) confirms that the ancient artisans were able to modulate the microstructure and the related properties as a function of the size of the nails and of their final applications.

ACKNOWLEDGEMENT

The authors desire to thank very much Mr. Piero Pellin for the performed SEM-EBSD analysis and Ing. Sebastiano Zorzi for his efforts in the preparation of the analysed samples.

REFERENCES

[1] R.F. Tylecote: A History of Metallurgy, Maney for the Institute of Metals, London, 1992, 63-63.
[2] R.F. Tylecote: J. Iron Steel Institute, 1 (1962), 19-22.
[3] H.F.Cleere: Bulletin of London University Institute of Archeology, 1 (1958), 55-74.
[4] N.S. Angus, G.T. Brown, H.F. Cleere: J. Iron Steel Inst., 11 (1962), 956-968.
[5] M.Boniardi, E.Gariboldi, M.Vedani: Metallurgical Science and Technology, 1 (1992), 28-38.
[6] Verein Deutscher Eisenhüttenleute: Sclackenatlas, Verlag Stahleisen, Düsseldorf, 1981.
[7] F. Oeters: Metallurgy of Steelmaking, Verlag Stahleisen, Düsseldorf, 1994, 26.
[8] C. Panseri: Ricerche Metallografiche Sopra una Spada da Guerra del XII Secolo", 1, Quad.1, AIM, Milano, 1954.
[9] H.Preβlinger, M. Mayr: Steel Research Int., 8 (2001), 283-290.
[10] H.Preβlinger, O.H. Urban, E. M. Ruprechtsbeger: Steel Research Int., 9 (2005), 666-671.
[11] C. Mapelli, W.Nicodemi, R.F.Riva: ISIJ Int, 7 (2007), 1049-1056.
[12] R.K. Ray, J.J.Jonas M.P. Butron-Guillen, J. Savie: ISIJ Int., 34 (1994), 927-942
[13] F.J. Humphreys, M. Hatherly: Recrystallization and Related Annealing Phenomena 2nd Ed. Amsterdam: Elsevier Ltd; 2004, 138-140.

ABSTRACT

CHIODI DEI LEGIONARI ROMANI RINVENUTI PRESSO INCHTUTHIL

Parole chiave: storia della metallurgia

Il presente articolo è focalizzato sullo studio di alcuni reperti provenienti da uno dei più famosi ed eclatanti ritrovamenti di componenti strutturali di età romana. I chiodi sono stati rinvenuti nel Pertshire, presso Inchthutil dove i legionari romani li abbandonarono nel 87 d.C. per evitare che cadessero nelle mani dei nemici. I chiodi presentano una struttura multistrato, con alternanza di regioni perlitiche e ferritiche (Fig. 1, Fig. 2, Fig. 3, Fig. 4, Fig. 5). Tale eterogeneità microstrutturale si riflette nella significativa variazione delle durezze misurate nelle diverse regioni del chiodo (Tab. 1, Tab. 2). Le inclusioni riscontrate all'interno dei chiodi sono di natura esogena e sono senza dubbio inclusioni di natura fayalitica saturate in ossido di ferro (Fig. 6, Fig. 7), che sono bassodondenti e furono con ogni probabilità elaborate per consentire di rivestire le superfici da forgiare a caldo, evitando l'ossidazione che avrebbe impedito di saldare tra loro le superfici dal blumo da cui i chiodi sono stati ricavati. L'analisi cristallografica delle tessiture presenti all'interno del chiodo (Fig. 8, Fig. 9, Fig. 10, Fig. 11, Fig. 12, Fig. 13), indica che vi è una rilevante presenza di fibra-γ. Questo fenomeno sembra suggerire che, seppure su basi empiriche, fu messo a punto un ciclo termo-meccanico in cui si eseguiva una deformazione plastica a caldo dove la trasformazione fra fase γ e fase α doveva aver luogo prima della ricristallizzazione della fase γ. D'altra parte la presenza di grani con crescita abnorme (Fig. 15) e la presenza intensa di bordi grano di tipo Σ3 e Σ13 sembra indicare che il materiale è stato mantenuto ad alta temperatura in fase feritica, tanto da portare ad un accrescimento significativo dei grani ferritici.